coatings

MDPI

Article

A Low-Temperature Alumina/Copper Diffusion Bonding Process using La-Doped Titanium Interlayers

Cherng-Yuh Su [1,2,3,*], Jia-Liang Huang [2], Po-Chun Chen [4], Hsin-Jung Yu [3], Dai-Liang Ma [5] and Bang-Ying Yu [5]

1 Additive Manufacturing Center for Mass Customization Production, National Taipei University of Technology, Taipei 10608, Taiwan
2 Department of Mechanical Engineering, National Taipei University of Technology, Taipei 106, Taiwan; facileness33@gmail.com
3 Institute of Manufacturing Technology, National Taipei University of Technology, Taipei 106, Taiwan; s.hsinjung.yu@gmail.com
4 Department of Materials and Mineral Resources Engineering, National Taipei University of Technology, Taipei 106, Taiwan; cpc@mail.ntut.edu.tw
5 Materials and Electro-Optics Research Division, National Chung-Shan Institute of Science & Technology, Taoyuan 32599, Taiwan; aridrdi@gmail.com (D.-L.M.); yubonnie1314@gmail.com (B.-Y.Y.)
* Correspondence: cysu@ntut.edu.tw; Tel.: +886-2-2771-2171

Received: 17 September 2018; Accepted: 1 November 2018; Published: 14 November 2018

Abstract: Ceramic-to-metal heterojunctions have been established to improve high-temperature stability for applications in aerospace and harsh environments. In this work, we employed low-temperature diffusion bonding to realize an alumina/Cu heterogeneous joint. Using a thin layer of lanthanum-doped titanium (La-doped Ti) to metallize the alumina surface, we achieved the bonding at a temperature range of 250–350 °C. We produced a uniform, thermally stable, and high-strength alumina/Cu joint after a hot-press process in vacuum. Signals from X-ray diffraction (XRD) suggested the successful diffusion of Ti and La into the alumina substrate, as Ti can easily substitute Al in alumina, and La has a better oxygen affinity than that of Al. The transmission electron microscopy and XRD results also showed the existence of Cu_xTi_yO phases without Cu_xTi_y or LaO_x. In addition, the bonding strength of alumina/copper hot-pressed at 250, 300, and 350 °C were 7.5, 9.8 and 15.0 MPa, respectively. The process developed in this study successfully lowered the bonding temperature for the alumina/copper joint.

Keywords: alumina/copper heterojunction; low-temperature diffusion bonding; thin-film pre-metallization

1. Introduction

Heterojunctions of ceramics and metals have received increased attention because of the requirements of high-temperature-resistant composite parts in aerospace or military fields. There are many welding techniques [1] of ceramics and metals that have been developed from traditional active brazing, which wet the interface by melting active metals [2]. Among them, the techniques of active soldering [3,4] and pre-metallization [5–7] attracted our attention, because of their low active temperature and good bonding behavior. Direct bonding of copper to alumina has been developed by an eutectic reaction of copper and cuprous oxide at 1050 °C [8]. Fu et al. used titanium with $Sn_{0.3}Ag_{0.7}Cu$ to bond copper and alumina at 620 °C [9]. The predictability and strength have been enhanced, based on low active energy, to form a good junction, suppressed intermetallics [10,11],

and residual stress [12,13]. However, there are still the challenges of incomplete junctions due to the formation of oxides that cause low diffusion bonding of ceramics and metals during the process [14]. The addition of rare-earth elements, such as cerium [15] and lanthanum [16], is a potential option to decrease the possibility of oxide formation and to increase the effective substitution of atoms at the interface. The high oxygen affinity of the solder significantly suppresses oxides or intermetallic compounds, and optimizes the bonding qualities with a few amounts of rare-earth elements. In addition, Lim et al. reported their study on the bonding mechanism of sputtered copper thin film on an alumina substrate [17]. This study demonstrated that the adhesion strength of the sputtered copper thin film on the alumina substrate was enhanced by their inter-diffusion. Thus, in this study, we improved the direct bonding of copper at a lower temperature range (250 to 350 °C) by combining the pre-metallization with a rare-earth element, lanthanum, in order to investigate the chemical and mechanical properties of the copper/alumina joint [18]. In general, the current method that combines a few amounts of rare earth elements in the titanium solder [19], and the pre-metallization process, have achieved the goal of lowering the temperature of diffusion bonding for the heterojunctions of ceramics and metals, which also enhances their bonding strength [20]. Despite growing interest in the influence of rare-earth elements on the microstructure and mechanical properties of bonds, the effects of La on the diffusion bonding of alumina/copper are yet to be elucidated. In this study, we exploited the affinity of La for oxygen, so as to decrease the temperature required to achieve diffusion bonding. Then, we also investigated the resulting microstructure, in order to elucidate the mechanism underlying the diffusion process and the mechanical properties of diffusion bonding. To summarize, the main objective of this study was to further lower the diffusion bonding temperature for heterojunctions of ceramics and metals, and to improve the bonding strength so as to achieve better properties.

2. Materials and Methods

2.1. Material and Diffusion Bonding Processes

Substrates of oxygen-free alumina ceramic and pure copper ($10 \times 10 \times 0.5$ mm^3) were cleaned using a solvent sequence of acetone, isopropanol, and ethanol, in order to remove the organic and other contaminants. The samples were then dried in a furnace at 70 °C. Prior to the metallization of the substrate, a Ti–0.5La (wt %) target was pre-sputtered using the sputtering parameters in Table 1, for a period of 5 min, so as to exclude the oxides from the surface and to obtain a homogenous coating on Alumina. Then, the copper/alumina joints were bonded using physical vapor deposition (PVD) to coat a Ti–0.5La interlayer, at 250, 300, or 350 °C and 25 MPa for 120 min, under 5.5×10^{-5} torr, in a vacuum hot-press machine. Thereafter, we investigated the effects of processing temperature on the microstructure and strength of the copper/alumina joints.

Table 1. The parameters of sputtering in present study.

Target	Ti–0.5 La (wt %)
Power (W)	150
Sputtering time (min)	24
Ambient pressure (torr)	2×10^{-6}
Working pressure (torr)	5.5×10^{-3}
Working distance (cm)	9
Sputtering rate (nm min^{-1})	20.83

2.2. Microstructure Characterizations

The microstructure of the pre-metallized and bonded samples was examined using field-emission scanning electron microscopy (FE-SEM; LEO 1530 Gemini FESEM, Carl Zeiss AG, Oberkochen, Germany). The characteristic peaks were used to investigate the phase formation in the Ti solder deposited on the alumina and copper substrates at 350 °C.

A transmission electron microscope (FEI-TEM, Tecnai F20 G2, Philips, Amsterdam, The Netherland) and qualitative elemental chemical mapping (EDS, X-Max, Oxford Instruments, Abingdon, UK) were employed to investigate the interface of the Ti-0.5La layer at the copper/alumina joint.

The X-ray diffraction (XRD) patterns of the as-deposited and annealed samples were obtained using an X-ray diffractometer (M03-XHF, MAC Science, Tokyo, Japan), with Cu Kα radiation (λ = 1.54 Å), and the diffractograms were collected at a scan rate of 2° min^{-1} and a 2θ range of 20° to 80°. The characteristic peaks were used to investigate the phase formation in the Ti solder deposited on the alumina and copper substrates at 350 °C.

2.3. Mechanical Properties

2.3.1. Hardness Tests

The hardness properties of the diffusion bonding samples were examined using Vicker's hardness testing, in order to measure the hardness values. The hardness test was conducted in three areas, alumina substrate, copper substrate, and reaction layer, with 50, 300, or 500 g force (gf), respectively, over a duration of 10 s, in order to measure the hardness. Five measurement results were then averaged so as to obtain a representative hardness value for the samples.

2.3.2. Adhesion Tensile Tests

In accordance with the ASTM-D4541 standards [21], we adopted adhesion tensile test (PosiTest AT-A, DeFelsko, New York, NY, USA) samples with a test size of 20 × 10 mm^2. Following the adhesion tensile test, the fracture surface of the diffusion bonding sample was divided into two surfaces of copper and alumina substrates, for further investigation. In addition, the fractured surfaces of the samples were observed using FE-SEM with energy-dispersive X-ray spectroscopy (EDS). However, it was also necessary to evaluate the underlying mechanism of fracture; hence, XRD (M03-XHF, MAC Science, Tokyo, Japan) was used to characterize the crystal structure and possible phases. Three measurement results were averaged to obtain a representative adhesion tensile value for the samples.

3. Results and Discussion

3.1. Microstructure Characterizations

The pre-metallization process resulted in the formation of uniform thin films of Ti–0.5La and pure copper, showing a strong inter-diffusion of elements that promoted bonding with the alumina substrate. To simulate the diffusion mechanisms between the Ti–0.5La interlayers and copper substrates, copper thin films were coated on the Ti–0.5La surface in advance. Figure 1 presents the cross-section images with insets of planar images and profiles of the EDS line-scan of pre-metallization Ti–0.5La thin films fabricated at 250, 300, and 350 °C. As shown in Figure 1a–c, the thickness of each thin film was approximately 400 nm. The top-view images, insets in Figure 1a–c, show that the grains in the as-deposited thin films did not vary with the processing temperature. The results of the EDS line-scan indicate the inter-diffusion of each element, resulting in a strong diffusion bonding between the alumina ceramic substrate and pre-metallization thin films. Figure 1d shows that thin films of pure copper were deposited uniformly over the Ti–0.5La thin films.

Figure 2 presents the XRD results of pre-metallization thin films deposited at 350 °C, indicating the formation of a Cu_xTi_y phase. Figure 2a presents the XRD results of Ti thin films deposited on an alumina substrate, which indicates that Ti did not form Al_xTi_y intermetallic compounds, i.e., only TiO_x and pure alumina were present. Figure 2b presents the XRD results of Ti thin films deposited on a pure copper substrate, indicating the formation of $CuTi_2$ intermetallic phases as well as TiO and pure copper.

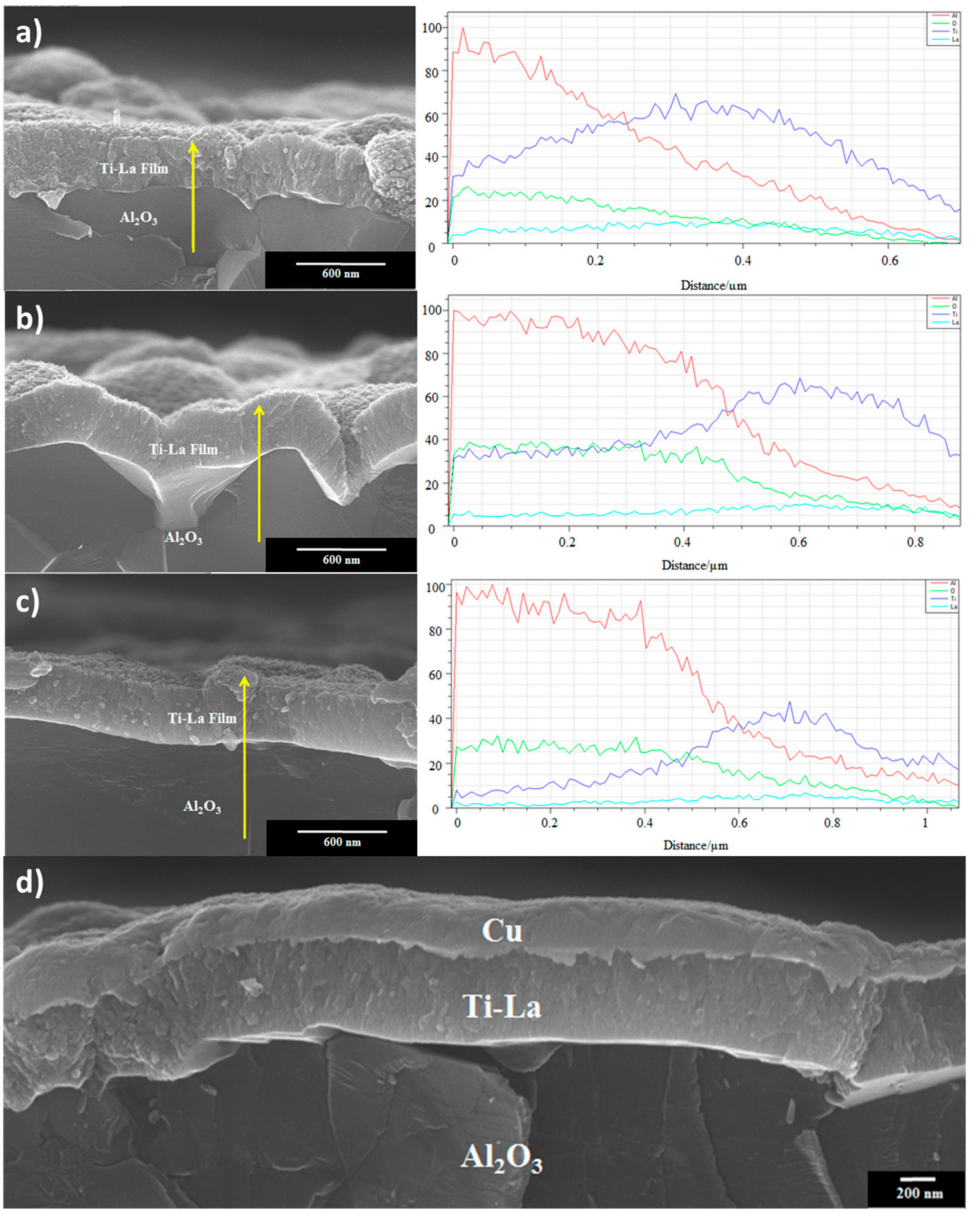

Figure 1. Cross-section images showing pre-metallization Ti–0.5La thin films on alumina substrates, with line scans. Samples were fabricated at process temperatures of (**a**) 250; (**b**) 300; and (**c**) 350 °C; (**d**) thin film of pure copper are deposited on the Ti–0.5La thin film.

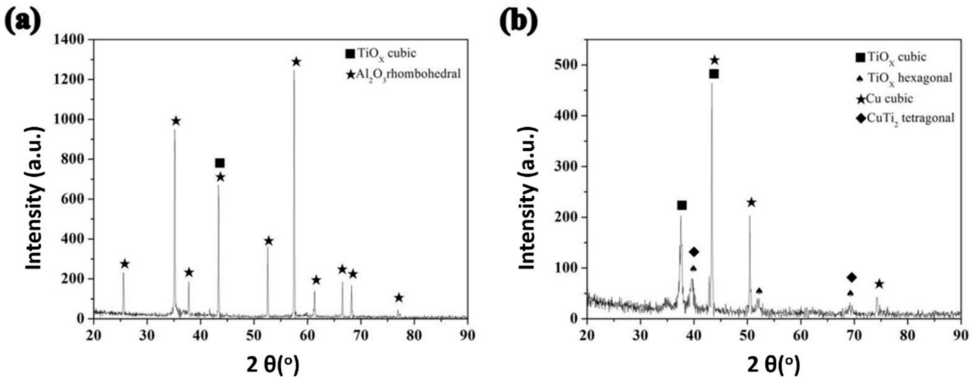

Figure 2. XRD analysis of Ti–0.5 La thin films deposited on (**a**) alumina and (**b**) copper substrates.

Low-temperature bonding could be induced using multiple pre-metallization layers, followed by the introduction of the rare-earth element, La. Firstly, a vacuum hot-pressing process was used to bond the copper substrate to the pre-metallized alumina substrate at 250, 300, and 350 °C. Figure 3 presents the cross-sectional SEM images and the profiles of the EDS line-scan of the copper/alumina joints processed at various temperatures. The black arrow in Figure 3 indicates the formation of a diffusion bonding zone (interlayer region) between the alumina and copper substrates, extending approximately 0.5 to 0.8 μm, without any defects. The results of the EDS line-scan indicate that the active elements (Ti and La) tend to aggregate on the alumina substrate, which is in accordance with Chang's report [22]. The roles of Ti and La in the diffusion bonding zone (interlayer region) have been shown. The migration of these elements is a clear indication of bonding with oxygen from the alumina substrate. Based on Howard et al. findings [23], the affinity of La for oxygen allows La to reduce the active energy of Al, and thereby promote diffusion bonding. Ti oxides do not form as readily as La oxides, because of their higher Gibbs energy; however, Ti retains the ability to wet the alumina surfaces through the substitution of Al to form strong bonds [24].

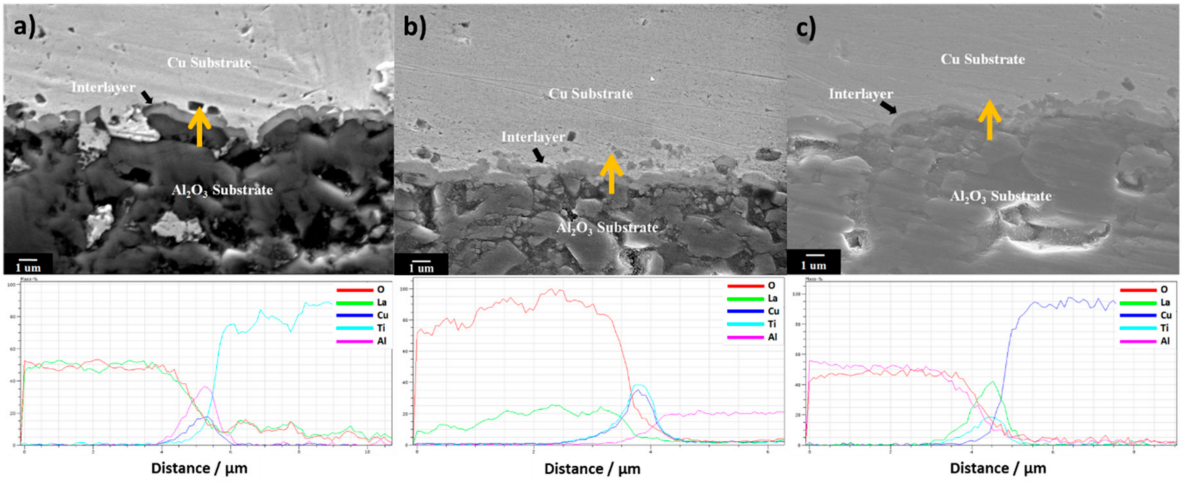

Figure 3. Cross-section images showing heterogeneous bonding of the alumina substrate and copper substrate, and line scans for various process temperatures: (**a**) 250, (**b**) 300, and (**c**) 350 °C.

TEM and EDS were employed to confirm the results of the composition and phase formation in the bonding layer formed at 350 °C. As shown in Figure 4, the bonding area can be divided into four layers, A, B, C, and D. The EDS results reveal that layer A comprises only alumina, whereas layer D comprises only the copper substrate. On the other hand, the EDS results of layers B and C (interlayers) reveal diffused Ti and O. This is a clear demonstration that La tends to diffuse into the alumina side rather than into the copper side. It shows that the TEM results are in agreement with the SEM results (see Figure 3). As indicated by the TEM images with diffraction patterns, layers A and D present a crystalline structure, whereas layers B and C present a poly-crystalline appearance. From these results, it can be assumed that layers A and D contain alumina and Cu_2O phases, respectively, whereas interlayers B and C contain TiO_2 and Ti_3Cu_3O, respectively. It is well-known that La can form oxides; however, this phase was not observed in the TEM images.

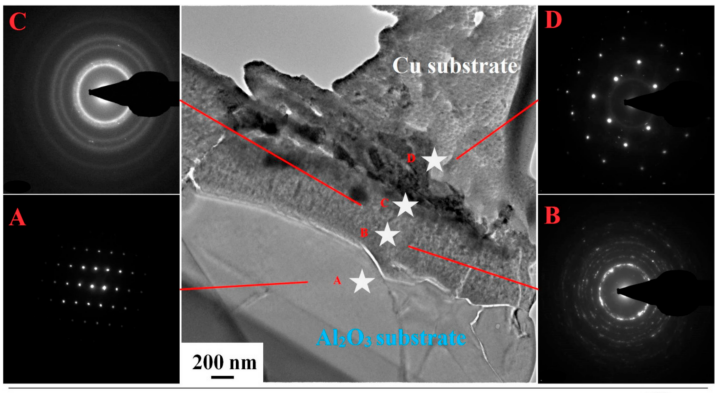

						at%
	Al	O	Ti	La	Cu	Possible phase
A	38.15	60.92	0.03	0.11	0.76	Al_2O_3
B	0.1	20.08	76.16	0.31	3.35	TiO_2
C	0.07	19	59.68	0.08	21.16	TiO_2, Ti_3Cu_3O
D	3.65	15.69	0.09	0.01	80.56	Cu_2O

Figure 4. TEM images and energy-dispersive X-ray spectroscopy (EDS) results showing the heterogeneous bonding of alumina and copper substrates fabricated at a process temperature of 350 °C.

3.2. Mechanical Properties

The hardness was independent of the process temperature, but the adhesion strength was proportional to the process temperature. The hardness and adhesion test results are presented in Figure 5. Firstly, Figure 5a shows the hardness results of different areas for the three process temperatures of 250, 300, and 350 °C. It indicates that the hardness varies at different areas, but not for different process temperatures, which suggests the difficulty in the formation of intermetallic compounds because of the low process temperature [25]. The large difference in hardness between the C and B areas suggests that such high differences in stiffness may influence the strength of the whole junction, and may result in rupture under external force. However, from Figure 5b, the results of the adhesion test indicate that the tensile strength was dependent on the process temperature, with average strengths of 7.5, 9.8, and 15.0 MPa after the 250, 300, and 350 °C processes, respectively. Therefore, the underlying mechanism may be ascribed to the micro-added La, which increases the bonding strength and welding capacity by decreasing the activation energy of element diffusion. The varying tensile strength of the diffusion bonding samples for the different process temperatures may be ascribed to less formation of intermetallic compounds and high diffusion bonding of Ti–0.5La (wt %), even with consistent hardness.

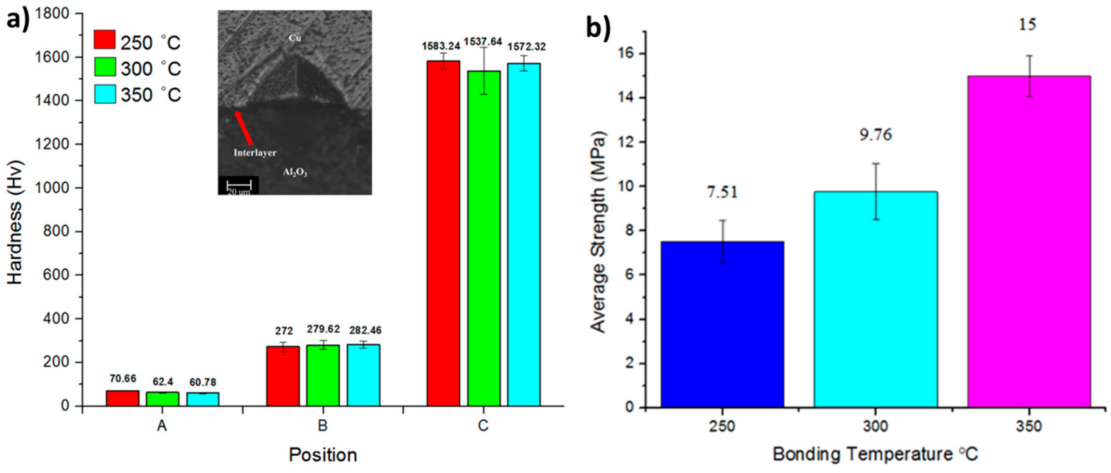

Figure 5. The (**a**) hardness at different areas, and (**b**) the tensile strength of the heterogeneous diffusion bondings of the alumina substrate and copper substrate for three different process temperatures, 250, 300, and 350 °C.

The fracture surfaces of the alumina and copper substrate sides were then closely examined using XRD, which is shown in Figure 6. The presence of alumina, TiO_2, $AlTi_3$, and Cu_3Ti_3O, according to JCPDS, is clearly shown in the XRD results in Figure 6a, and it contributed to the high O affinity of Ti, rather than Al. Therefore, from the literature [26], because of the high diffusion rate of O and the high O affinity of Ti, TiO_2 firstly formed, and then the remaining Al with a lower diffusion rate formed Ti_xAl_y. On the other hand, among the electronegative elements, Ti has a higher difference in electronegativity from O in the alumina than copper during the bonding process. Hence, O firstly diffused to the Ti–0.5La (wt %) solder to combine with Ti. Figure 6b presents many phase formations, including Cu, Cu_2O, $CuTi_3$, Ti, TiO_2, and Cu_3LaO_2, according to JCPDS. This indicated that a part of the Ti did not directly diffuse to the alumina substrate side, but diffused to the copper substrate side. Furthermore, the Cu_3LaO_2 characteristic peak was found at 48 °C, and may have formed from Cu_2O and La_2O_3 [27]. The underlying mechanism can be that La firstly formed oxides and then interacted with the cuprous oxide to from this ternary phase.

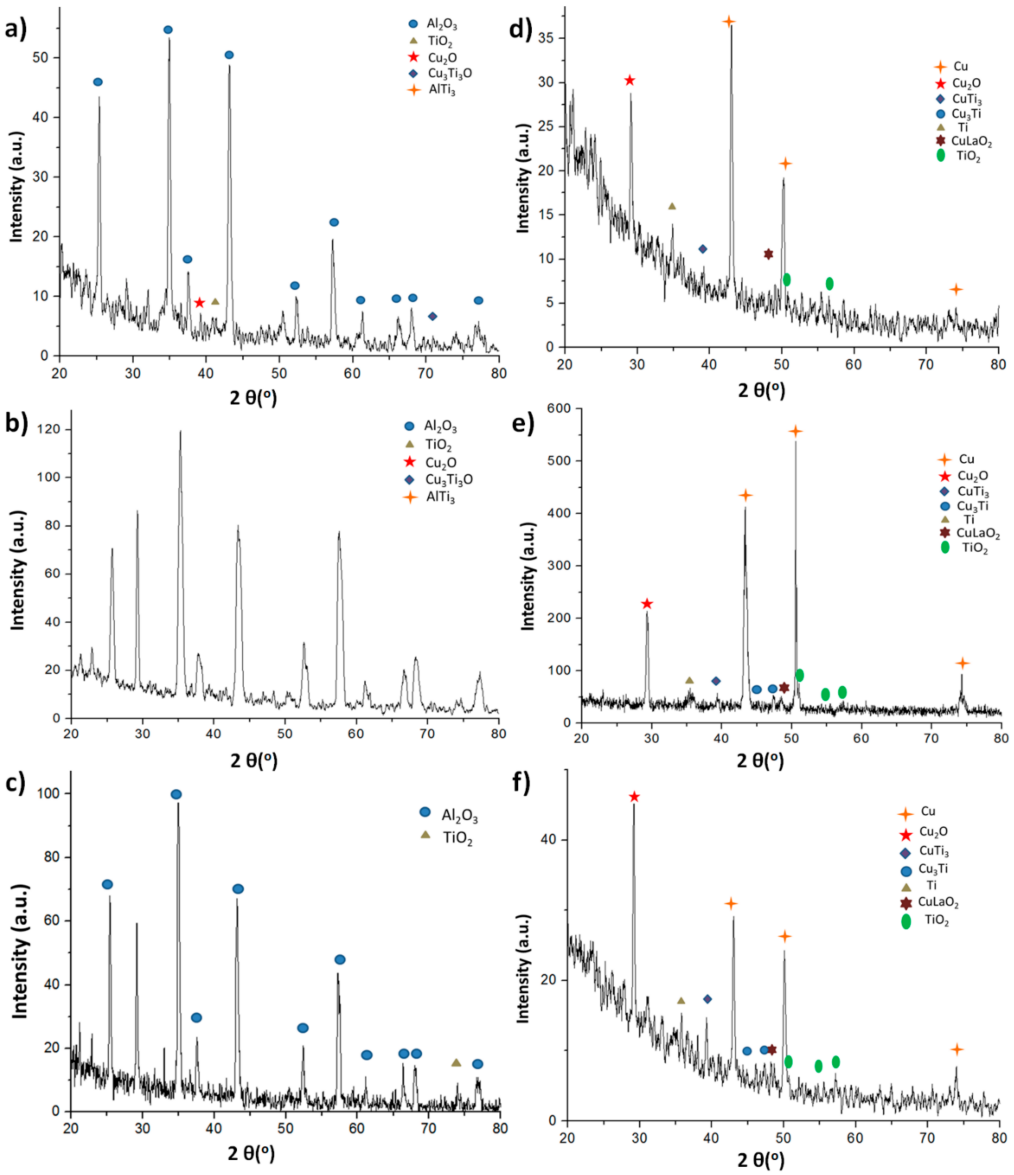

Figure 6. XRD analysis of fracture surface of alumina substrate side bonded at (**a**) 250 °C, (**b**) 300 °C, and (**c**) 350 °C; fracture surfaces of copper side bonded at (**d**) 250 °C, (**e**) 300 °C, and (**f**) 350 °C processes.

The morphologies of the fracture surfaces are shown in Figure 7, which presents each copper and alumina substrate side for the three process temperatures corresponding with the detailed compositions presented in Table 2. Based on the results in Figure 7 and Table 2, the surfaces of the alumina and copper substrate side all contained both convex and concave areas (indicated by A and B marks), but with differing compositions. Figure 7a–c shows that the fracture surfaces from the alumina substrate side all have a similar Cu_xTi_yO composition at area A. However, area B has the same alumina composition in the 250 and 300 °C samples, but a CuTiO ternary phase in the 350 °C sample. In summary, the concave area of B indicates that there is an interaction layer near the alumina substrate side; therefore, there are some layers that broke and remained on it after the tensile test. On the other hand, Figure 7d–f shows that the fracture surfaces from the copper substrate side all have similar TiO and CuO compositions in areas A and B. The combined results of XRD, shown in Figure 2, and SEM indicate that the white areas in Figure 7a–c may be the CuTiO phases.

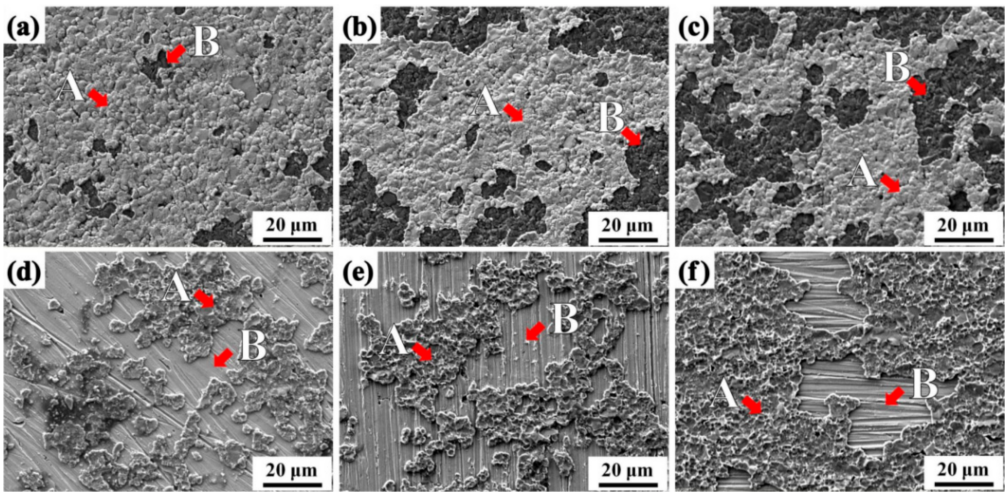

Figure 7. SEM fracture surface of heterogeneous diffusion bonding on (**a**–**c**) alumina substrate side and (**d**,**e**) copper substrate side under 250, 300, and 350°C hot vacuum process, respectively.

Table 2. EDS results of elemental compositions (at %) of area A and B in each fracture surface of the alumina and copper substrate side under 250, 300, and 350 °C processes, respectively.

Samples	Area	O (at %)	Al (at %)	Ti (at %)	Cu (at %)
250 °C alumina	A	9.47	0.12	5.53	84.89
	B	67.32	31.21	1.16	0.31
250 °C Cu	A	48.78	0.01	47.58	3.64
	B	4.05	0.13	0.07	95.75
300 °C alumina	A	4.38	0.26	6.77	88.58
	B	67.82	31.01	0.98	0.18
300 °C Cu	A	32.09	0.34	65.53	2.03
	B	2.33	–	–	97.67
350 °C alumina	A	3.99	0.37	3.52	92.11
	B	15.55	3.55	26.75	54.16
350 °C Cu	A	40.87	0.18	56.47	2.48
	B	–	0.01	0.60	99.39

4. Conclusions

A low-temperature diffusion bonding process to create a heterogeneous joint between alumina and copper was successfully demonstrated in this work. We successfully lowered the hot-press temperature to 350 °C by doping a rare earth element in the pre-metallization layer of Ti. Based on

the microstructural characterization, we realized that the hot-press temperature did not significantly influence the grain size, and that hardness did not vary with the hot-press temperature. The hot-press temperature influenced the tensile strength of the heterogeneous bonding, which depended on the La doping. In addition, La and Ti diffusion into alumina improved the bonding strength, as Ti can substitute Al in alumina, and La has a high oxygen affinity. Moreover, XRD indicated that the phases formed in the copper substrate are more than those in the alumina substrate side. Ti has a higher diffusion coefficient than O, a high O affinity, and has a direct diffusion path to alumina, all of which make it conducive to making the low-temperature diffusion bonding of alumina and copper possible.

Author Contributions: Conceptualization, C.-Y.S.; Formal Analysis, C.-Y.S. and P.-C.C.; Funding Acquisition, D.-L.M.; Investigation, C.-Y.S. and P.-C.C.; Methodology, P.-C.C.; Project Administration, C.-Y.S.; Resources, C.-Y.S. and D.-L.M.; Supervision, C.-Y.S. and D.-L.M.; Validation, J.-L.H., H.-J.Y., and B.-Y.Y.; Writing-Original Draft Preparation, J.-L.H. and P.-C.C.; Writing-Review & Editing, C.-Y.S. and P.-C.C.

Funding: This research was funded by the "Additive Manufacturing Center for Mass Customization Production" from The Featured Areas Research Center Program within the framework of the Higher Education Sprout Project by the Ministry of Education (MOE) in Taiwan. In addition, the authors would like to thank the Chung-Shan Institute of Science and Technology of the Republic of China (No. NCSIST-622-V102 (107)) and the Ministry of Science and Technology of Taiwan (MOST) (No. 106-2221-E-027-056-MY2 and 106-2623-E-027-001-D) for the financial support of this research.

Conflicts of Interest: The authors declare no conflict of interest. The funders had no role in the design of the study; in the collection, analyses, or interpretation of data; in the writing of the manuscript; or in the decision to publish the results.

References

1. Zhang, Y.; Di, F.; He, Z.-Y.; Chen, X.-C. Progress in joining ceramics to metals. *J. Iron Steel Res. Int.* **2006**, *13*, 1–5. [CrossRef]
2. Simões, S.; Ramos, A.; Viana, F.; Vieira, M.; Vieira, M. Joining of tial to steel by diffusion bonding with Ni/Ti reactive multilayers. *Metals* **2016**, *6*, 96. [CrossRef]
3. Smith, R.W. Active solder joining of metals, ceramics and composites: Brazing and soldering. *Weld. J.* **2001**, *80*, 30–35.
4. Chuang, C.-H.; Lin, Y.-C.; Lin, C.-W. Intermetallic reactions during the solid-liquid interdiffusion bonding of Bi2Te2.55Se0.45 thermoelectric material with Cu electrodes using a Sn interlayer. *Metals* **2016**, *6*, 92. [CrossRef]
5. Zheng, C.; Lou, H.; Fei, Z.; Li, Z. Partial transient liquid-phase bonding of Si_3N_4 with Ti/Cu/Ni multi-interlayers. *J. Mater. Sci. Lett.* **1997**, *16*, 2026–2028. [CrossRef]
6. Hongqi, H.; Yonglan, W.; Zhihao, J.; Xiaotian, W. Interfacial reaction of alumina with Ag-Cu-Ti alloy. *J. Mater. Sci.* **1995**, *30*, 1233–1239. [CrossRef]
7. Jadoon, A.K.; Ralph, B.; Hornsby, P.R. Metal to ceramic joining via a metallic interlayer bonding technique. *J. Mater. Process. Technol.* **2004**, *152*, 257–265. [CrossRef]
8. Yoshino, Y. Role of oxygen in bonding copper to alumina. *J. Am. Ceram. Soc.* **1989**, *72*, 1322–1327. [CrossRef]
9. Fu, W.; Song, X.G.; Hu, S.P.; Chai, J.H.; Feng, J.C.; Wang, G.D. Brazing copper and alumina metallized with Ti-containing Sn0.3Ag0.7Cu metal powder. *Mater. Des.* **2015**, *87*, 579–585. [CrossRef]
10. Yilbaş, B.S.; Şahin, A.Z.; Kahraman, N.; Al-Garni, A.Z. Friction welding of St Al and Al Cu materials. *J. Mater. Process. Technol.* **1995**, *49*, 431–443. [CrossRef]
11. Abbasi, M.; Taheri, A.K.; Salehi, M. Growth rate of intermetallic compounds in Al/Cu bimetal produced by cold roll welding process. *J. Alloy Compd.* **2001**, *319*, 233–241. [CrossRef]
12. Lanin, A. Effect of residual stresses on the strength of ceramic materials (Review). *Rus. Metall. Met.* **2012**, *2012*, 307–322. [CrossRef]
13. Bartlett, A.; Evans, A.; Rühle, M. Residual stress cracking of metal/ceramic bonds. *Acta Metall. Mater.* **1991**, *39*, 1579–1585. [CrossRef]
14. Hynes, N.R.J.; Velu, P.S.; Kumar, R.; Raja, M.K. Investigate the influence of bonding temperature in transient liquid phase bonding of SiC and copper. *Ceram. Int.* **2017**, *43*, 7762–7767. [CrossRef]

15. Wang, J.-X.; Xue, S.-B.; Han, Z.-J.; Yu, S.-L.; Chen, Y.; Shi, Y.-P.; Wang, H. Effects of rare earth Ce on microstructures, solderability of Sn–Ag–Cu and Sn–Cu–Ni solders as well as mechanical properties of soldered joints. *J. Alloy Compd.* **2009**, *467*, 219–226. [CrossRef]
16. Wang, S.; Zhou, H.; Kang, Y. The influence of rare earth elements on microstructures and properties of 6061 aluminum alloy vacuum-brazed joints. *J. Alloy Compd.* **2003**, *352*, 79–83. [CrossRef]
17. Lim, J.D.; Lee, P.M.; Chen, Z. Understanding the bonding mechanisms of directly sputtered copper thin film on an alumina substrate. *Thin Solid Films* **2017**, *634*, 6–14. [CrossRef]
18. Xia, Z.; Chen, Z.; Shi, Y. Effect of rare earth element additions on the microstructure and mechanical properties of tin-silver-bismuth solder. *J. Electron. Mater.* **2002**, *31*, 564–567. [CrossRef]
19. Kim, J.-H.; Kim, D.S.; Lim, S.T.; Kim, D.K. Interfacial microstructure of diffusion-bonded SiC and Re with Ti interlayer. *J. Alloy. Compd.* **2017**, *701*, 316–320. [CrossRef]
20. Wu, C.M.L.; Yu, D.Q.; Law, C.M.T.; Wang, L. Properties of lead-free solder alloys with rare earth element additions. *Mater. Sci. Eng. R Rep.* **2004**, *44*, 1–44. [CrossRef]
21. *ASTM D4541 Standard Test Method for Pull-Off Strength of Coatings Using Portable Adhesion Testers*; ASTM International: West Conshohocken, PA, USA, 2010.
22. Chang, S.; Chuang, T.; Tsao, L.; Yang, C.; Yang, Z. Active soldering of ZnS–SiO_2 sputtering targets to copper backing plates using an $Sn_{3.5}Ag_4Ti$ (Ce, Ga) filler metal. *J. Mater. Process. Technol.* **2008**, *202*, 22–26. [CrossRef]
23. Howard, S.M. *Ellingham Diagrams*; SD School of Mines and Technology: Rapid City, SD, USA, 2006.
24. Tsao, L. Interfacial structure and fracture behavior of 6061 Al and MAO-6061 Al direct active soldered with Sn–Ag–Ti active solder. *Mater. Des.* **2014**, *56*, 318–324. [CrossRef]
25. Kassner, M.; Tolle, M.; Rosen, R.; Henshall, G.; Elmer, J. Discussion of void nucleation. *Metall. Trans. A* **1993**, *24*, 1877–1878. [CrossRef]
26. Zalar, A.; Baretzky, B.; Hofmann, S.; Rühle, M.; Panjan, P. Interfacial reactions in Al_2O_3/Ti, Al_2O_3/Ti_3Al and Al_2O_3/TiAl bilayers. *Thin Solid Films* **1999**, *352*, 151–155. [CrossRef]
27. Jacob, K.T.; Jayadevan, K.P. Phase relations in the system Cu-La-O and thermodynamic properties of $CuLaO_2$ and $CuLa_2O_4$. *J. Mater. Sci.* **2002**, *37*, 1611–1620. [CrossRef]